Manuscript Details

Manuscript number	EST_2018_354
Title	Performance of recovered and reagent grade electrolyte in a soluble lead redox cell
Article type	Research Paper

Abstract

This paper presents the performance of ‘recovered’ electrolyte for the soluble lead flow battery, made by recycling conventional lead-acid battery electrodes, and compares it to reagent grade electrolyte for the same system. The two electrolyte compositions were cycled in static and flow cells and their charge, energy, and voltage efficiencies compared. The average charge, energy, and voltage efficiencies of static cells using 1.0 mol·dm^{-3} Pb^{2+} recovered electrolyte were 89%, 86%, and 96%, while cells using reagent grade electrolyte averaged 63%, 49%, and 78%, respectively. The average charge efficiency of flow cells with recovered electrolyte was consistently above 80% and within 10% of the average for cells with reagent grade electrolyte. The average energy and voltage efficiencies were 62% and 73%, respectively, diverting from averages for the reagent grade electrolyte cells by less than 15%. The highest average cycle life was for cells with recovered electrolyte at 187 cycles, while that of cells with reagent grade electrolyte peaked at 102. Trace elements in both electrolyte compositions were analysed and their presence in the recovered electrolyte appears to enhance performance of the soluble lead cells. The recovered electrolyte is an electrochemically viable substitute for the reagent grade electrolyte.

Keywords	soluble lead flow battery; recovered electrolyte; expended battery electrodes

Corresponding Author	Keletso Orapeleng
Corresponding Author's Institution	University of Southampton
Order of Authors	Keletso Orapeleng, Richard Wills, Andrew Cruden

Submission Files Included in this PDF

File Name [File Type]

Cover letter Keletso Orapeleng.docx [Cover Letter]

Highlights.docx [Highlights]

Performance of recovered and reagent grade electrolyte in a slrc.docx [Manuscript File]

To view all the submission files, including those not included in the PDF, click on the manuscript title on your EVISE Homepage, then click 'Download zip file'.

Energy Technology Research Group
Faculty of Engineering and the Environment
University of Southampton
SO17 1BJ
Southampton, UK
04th July 2018

Journal of Energy Storage Editorial Office

Subject: Submission of a Research Article for evaluation

Dear Editor,

I am enclosing a Research Article titled “Performance of recovered and reagent grade electrolyte in a soluble lead redox cell”, based on original research, for evaluation and eventual publication in your esteemed journal.

In this paper we compare a novel electrolyte we developed for a soluble lead battery with a conventional reagent grade electrolyte. The novel electrolyte performs just as well in a soluble lead flow battery as reagent grade electrolyte. This is significant because the novel electrolyte is made from end-of-life lead acid battery electrodes in a way that is significantly less energy intensive than traditional methods, hence proving a low cost alternative for emerging technology of redox flow batteries. This research may be of interest to those working on the soluble lead redox flow battery as well as those seeking innovative ways to harvest led out of lead acid batteries in a sustainable manner.

Neither the manuscript nor the contents have been published or are under consideration for publication in another journal.

Thank you for your consideration of our work. Please address all correspondence regarding this manuscript to me at ko1d13@soton.ac.uk.

Yours faithfully,

Ms. Keletso Orapeleng

Attachments:

MSWord manuscript
MSWord highlights

Highlights

This paper:

- Presents trace element analysis of reagent grade and recovered electrolytes for the soluble lead flow battery,
- Compares electrochemical performance of electrolytes manufactured from reagent grade and recovered materials,
- Highlights the importance of trace (< 1 mg·dm^{-3}) elements on performance of the soluble lead flow battery electrolytes,
- Identifies recycled lead-acid cells as a source of active material for the soluble lead flow battery.

List of Tables

List of Figures

Title: Performance of recovered and reagent grade electrolyte in a soluble lead redox cell

Authors: Keletso Orapeleng*; Richard G.A. Wills; Andrew Cruden

ko1d13@soton.ac.uk; rgaw@soto.ac.uk; a.j.cruden@soton.ac.uk

Energy Technology Group, University of Southampton, Southampton SO17 IBJ, UK

*Corresponding author: ko1d13@soton.ac.uk; Energy Technology Group, University of Southampton, Southampton SO17 IBJ, UK.

Abstract

This paper presents the performance of 'recovered' electrolyte for the soluble lead flow battery, made by recycling conventional lead-acid battery electrodes, and compares it to reagent grade electrolyte for the same system. The two electrolyte compositions were cycled in static and flow cells and their charge, energy, and voltage efficiencies compared. The average charge, energy, and voltage efficiencies of static cells using 1.0 mol·dm^{-3} Pb^{2+} recovered electrolyte were 89%, 86%, and 96%, while cells using reagent grade electrolyte averaged 63%, 49%, and 78%, respectively. The average charge efficiency of flow cells with recovered electrolyte was consistently above 80% and within 10% of the average for cells with reagent grade electrolyte. The average energy and voltage efficiencies were 62% and 73%, respectively, diverting from averages for the reagent grade electrolyte cells by less than 15%. The highest average cycle life was for cells with recovered electrolyte at 187 cycles, while that of cells with reagent grade electrolyte peaked at 102. Trace elements in both electrolyte compositions were analysed and their presence in the recovered electrolyte appear to enhance performance of the soluble lead cells. The recovered electrolyte is an electrochemically viable substitute for the reagent grade electrolyte.

Keywords: soluble lead flow battery, recovered electrolyte, expended battery electrodes

1. Introduction

It is anticipated that the utilisation of electrical energy storage systems will be critical for high penetration levels (i.e. >50%) of renewable energy, as currently envisaged in many countries' energy plans [1]. Within the megawatt (MW+) electrical energy storage technology sector, redox flow batteries are emerging as a viable option for enabling renewable energy penetration [2] and are expected to become commercially competitive [3].

The soluble lead cell using methanesulfonic acid as electrolyte was introduced by [Pletcher et al. 4, 5-10] using the redox couples PbO_2/Pb^{2+} and Pb/Pb^{2+}, on the positive and negative electrodes respectively. The electrolyte provides the Pb^{2+} ions, which are electrochemically converted to solid PbO_2 and Pb and deposited on the positive and negative electrodes respectively during charge, and stripped back into electrolyte as soluble ions during discharge. The reactions are as follows [4, 11].

Positive electrode

$$PbO_2 + 4H^+ + 2e^- \overset{\text{discharge}}{\rightarrow} Pb^{2+} + 2H_2O \qquad E^o = 1.460\ \text{V} \qquad (1)$$

Negative electrode

$$Pb \overset{\text{discharge}}{\rightarrow} Pb^{2+} + 2\,e^- \qquad E^o = -0.126\ \text{V} \qquad (2)$$

Overall

$$Pb + PbO_2 + 4H^+ \overset{\text{discharge}}{\rightarrow} 2Pb^{2+} + 2H_2O \qquad E_{cell} = 1.586\ \text{V} \qquad (3)$$

The choice of acid for making electrolyte for the soluble lead flow battery (SLFB) is dependent on lead (II) ion solubility. Other factors include ionic conductivity needed to

transfer ions between the electrolyte and the deposit, a low electrical conductivity that prevents electrical losses, stability at the operation voltages, and at operation temperature. Low toxicity, corrosiveness and volatility are also critical. Ideally, the chemicals used to make the electrolyte should also be low cost and easy to obtain. In practice it is difficult to find an electrolyte that possesses all these qualities. Therefore a compromise is often found.

In the Table 1 below methanesulfonic acid (MSA) compares favourably with other acids for making Pb^{2+} electrolyte. Solubility of Pb^{2+} is highest in methanesulfonate at 2.6 $mol \cdot dm^{-3}$ [12]. MSA costs the least (Sigma Aldrich prices as at 06/2018), and is the least corrosive. MSA is also stable at an acceptable range of temperatures and at the operation voltage of 0 – 2.0 V. Even though its ionic conductivity is lower compared to the other three acids, it is still acceptably high.

Table 1: Comparison of common acids used as electrolytes on lead solvation, ionic conductivity, corrosiveness and cost.

Acid	$[Pb^{2+}]$ / $mol \cdot dm^{-3}$	Ionic Conductivity in 1N Acid / $S \cdot cm^2 \cdot mol^{-1}$	Corrosive	Stable at Tempera T / °C	Cost (S.Aldrich)	At purity (S.Aldrich)
MSA	2.600	299.60 [12]	No	17 – 167	£44.10/L	(70%)
Sulfuric acid	0.0001	444.88 [12]	Highly corrosive	10 – 300	£66.00/L	(95-98%)
Hydrochloric acid	0.034	346.11 [12]	Corrosive	-30 – 61	£372.00/L	(36.5-38%)
Nitric acid	1.803	370.00	Highly corrosive	-42 – 83	£239.00/L	(70%)

1.1. Reagent Grade Soluble Lead Flow Battery Electrolyte

Reagent grade electrolyte (RGE) for the SLFB is made from high purity lead methanesulfonate (462667 Aldrich) and methanesulfonic acid (471348 Sigma Aldrich). Existing literature indicates that different concentrations of the Pb^{2+} ions and of the acid have been tested to determine effects on operation of the soluble lead cell [4, 6]. Li *et al.* [13] found that low concentration of Pb^{2+} (0.1 mol·dm^{-3}) in electrolyte resulted in a powdery deposit on the positive electrode, which contributes to accumulation of solids on the positive electrode and consequently, on the negative electrode as well. [Hazza *et al.*4] showed that the higher the concentration of acid, the higher the conductivity of the electrolyte, while at the same time recommending a maximum acid concentration of 2.0 mol·dm^{-3} to prevent reaching the solubility limit of Pb^{2+} in methanesulfonate. They also recommended the same acid concentration to prevent deposit cracking on the positive electrode [10]. A higher concentration of Pb^{2+} (0.7 mol·dm^{-3}) is recommended [14] in order to store practical amounts of energy and optimise electrochemical activity. Based on these considerations, electrolytes with a Pb^{2+} concentration of 0.9 mol·dm^{-3}, 1.0 mol·dm^{-3} MSA [9] and 0.7 mol·dm^{-3}, 1.0 mol·dm^{-3} MSA [14] have been recommended.

In this paper we present results comparing the reagent grade electrolyte (RGE) typically used for the SLFB with a recycled electrolyte (RE) prepared from discarded Starting, Lighting and Ignition (SLI) lead acid batteries. The use of such a recycling process would provide an alternative materials source for further development of the SLFB.

2. Experimental

A comparison of RGE and RE based on several performance criteria have been carried out to asses efficacy of the RE. Comparison criteria focussed on performance evaluation of both electrolytes in a soluble lead static cell (SLSC) and a soluble lead flow cell (SLFC).

To assess performance in an electrochemical energy storage cell, criteria outlined by Ponce de Leon [2] was used. In these criteria, standard parameters suitable for evaluating different battery technologies were used. These are charge, energy, and voltage efficiencies. These help to normalise the performance of different technologies and different size cells, making it possible to compare dissimilar batteries:

$$\text{Voltage efficiency, } \eta_V = \frac{V_{cc}(Discharge)}{V_{cc}(Charge)} \quad (4)$$

$$\text{Charge efficiency, } \eta_C = \frac{Q(Discharge)}{Q(Charge)} \quad (5)$$

$$\text{Energy efficiency, } \eta_e = \frac{E(Discharge)}{E(Charge)} \quad (6)$$

$$\text{Power efficiency, } \eta_P = \frac{IV_{cc}(Discharge)}{IV_{cc}(Charge)} \quad (7)$$

To compare the above parameters, the electrolytes were galvanostatically cycled in a 5 cm x 5 cm SLSC and in a 4 cm x 2.5 cm SLFC. Battery cycle life, which is an important indicator of battery life and has implications on lifetime costs of a storage system, was determined for both cell types.

2.1. Recovered Soluble Lead Flow Battery Electrolyte

Recovered electrolyte (RE) was prepared using electrodes from a spent 7 Ah, 12V Valve Regulated Lead Acid (VRLA), Yuasa NP7-12L battery in methanesulfonic acid and hydrogen

peroxide. The electrodes were crushed into solids of rough diameter 10^{-4} - 10^{-3} m and used as the solute in 2.5 mol·dm^{-3} methanesulfonic acid. To aid reduction of the PbO_2 and oxidation of Pb into Pb^{2+} ions, 0.1 mol·dm^{-3} hydrogen peroxide was added [15] (p600). The reactions are:

$$PbO_2 + H_2O_2 + 2CH_3SO_3H \rightarrow Pb(CH_3SO_3)_2 + 2H_2O + O_2 \quad (8)$$

$$Pb + H_2O_2 + 2CH_3SO_3H \rightarrow Pb(CH_3SO_3)_2 + 2H_2O \quad (9)$$

A full description of the method used to make recovered electrolyte is covered in [16].

The composition of the recovered electrolyte, analysed using Inductively Coupled Plasma Mass Spectroscopy, is given in the Table 2. Inductively Coupled Plasma Mass Spectroscopy

2.2. Equipment

An eight channel battery analyser by MTI Corporation was used for galvanostatic cycling. The electrochemical battery analyser was connected to a laptop with software that allowed control of experiments as well as recording of the data as the experiment progressed. During flow cell electrochemical tests, a Watson Marlow 505S peristaltic pump was used to circulate electrolyte for the soluble flow cell.

2.3. Test Cells

2.3.1. Static Cell

A static cell was made of two 5 cm x 5 cm x 2 mm SIGRACELL graphite electrodes. The electrodes were separated by a silicone insulator, which created a 5 cm x 5 cm x 5 mm cell chamber in which electrolyte was collected. The silicone gaskets also provided insulation

against electrolyte leaks. A 5cm x 5 cm x 0.1 mm thick nickel foil was placed flush against the back of each electrode to act as a current collector. Silicone gaskets were used to insulate the cell's conductive parts from the clamps that held the cell together. The current collectors were connected to the battery analyser leads. The cell had an active area of 25 cm^2 on each electrode. The cell-gap was maintained at 8 mm. The cell is shown in Figure 1.

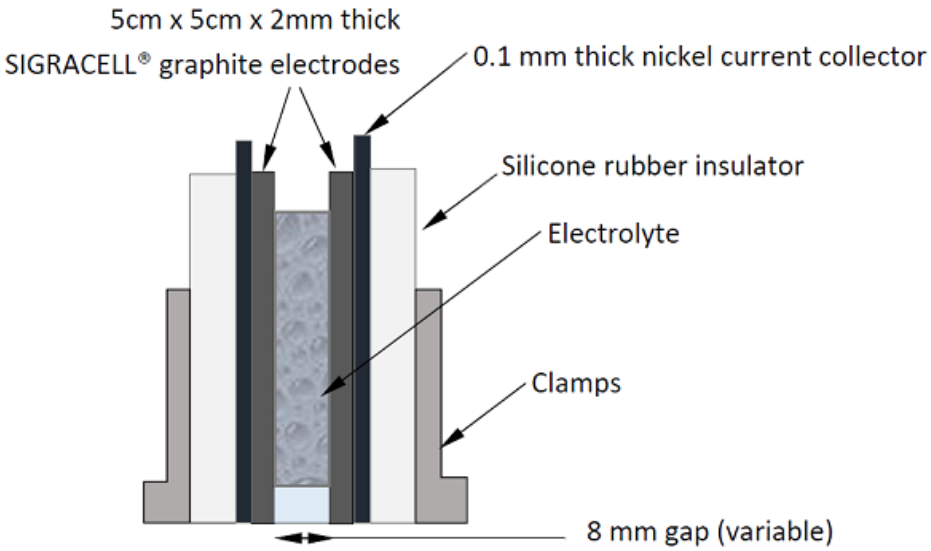

Figure 1: Cross section of static soluble lead cell. The static cell has a 5cm x 5cm x 5mm wide cell chamber with two 5cm x 5cm x 0.2cm graphite electrodes on either side. 0.1 mm thick nickel foils are placed against each electrode to collect current from the electrodes. The whole cell is held together by clamps and insulated with silicone rubber to minimise leakage.

2.3.2. Flow Cell

The soluble lead flow cell, shown in Figure 2, is made of a polyvinyl chloride (PVC) backing board which gives the cell structural support. Silicone rubber sheets isolate the functional parts of the cell. The cell had 5.0 cm x 4.0 cm x 2.0 mm thick carbon polymer electrodes. A 5.0 cm x 4.0 cm x 0.1 mm thick nickel foil was used to collect current from each electrode. Two acrylic cell chambers provided a 4.0 cm x 2.5 cm by 2 cm half-cell chamber either side of a VPX-20 anion exchange membrane. Each of the acrylic chambers had an inlet and an

outlet through which electrolyte entered and left the cell. The electrolyte was circulated between the reservoir and the cell using Watson Marlow 505S peristaltic pumps and Masterflex Norprene tubes. An Erlenmeyer flask was used as a single electrolyte reservoir. Since the electrolyte from either side of the cell went into the same tank, the cell was classified as semi-divided. The setup is shown in Figure 3.

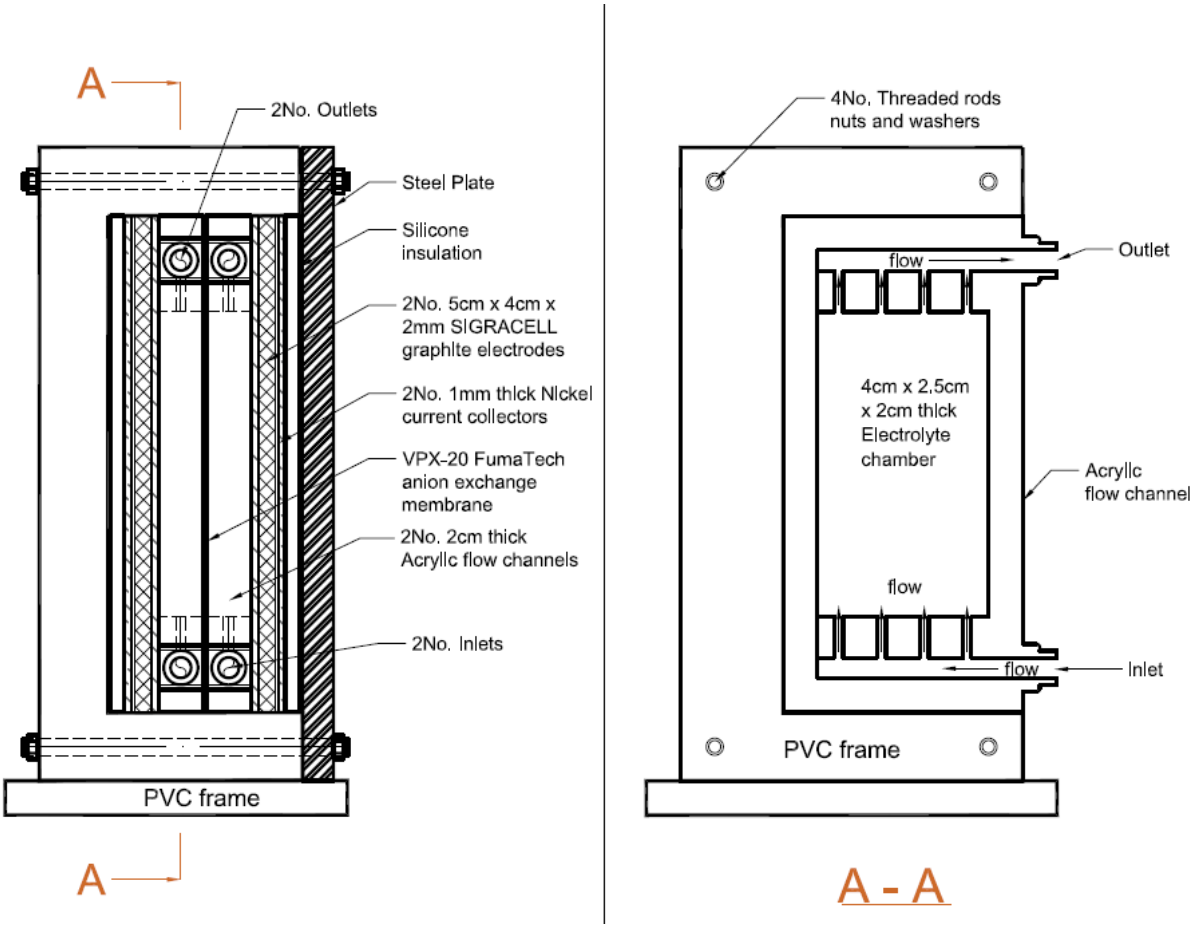

Figure 2: A soluble lead flow cell made of a structural PVC backing board, silicone spacers to isolate the functional parts of the cell, and 5.0 cm x 4.0 cm x 2.0 mm thick SIGRACELL carbon electrodes. 0.1 mm thick nickel foils were used as current collectors. 2No. acrylic cell chambers provided a 4 cm x 2.5 cm by 2.0 cm half-cell chamber either side of a VPX-20 anion exchange membrane. Each acrylic chamber had an inlet and outlet through which electrolyte entered and left the cell.

2.4. Measurements

2.4.1. Elemental Analysis of Recovered Electrolyte

The data sheets of lead acid batteries used to make recovered electrolyte indicate that the battery electrodes contain calcium and antimony lead alloys (data sheets). This is to be expected since it is standard to alloy the refined lead used in lead acid batteries during recycling [17]. Apart from the alloying metals, refined lead also contains trace elements, some of which may be controlled during refining according to battery manufacturer's requirements. In order to determine the composition of recovered electrolyte made from the expended batteries, Inductively Coupled Plasma Mass Spectroscopy was conducted on a Thermo Scientific iCAP RQ ICP MS analyser. The samples were identified and quantified against available standards. Three samples were analysed for each element and the reported results are averaged between the three results.

2.4.2. Charge, Voltage and Energy Efficiency in Static Cells

The static soluble lead cell shown in Figure 1 was assembled and connected to the MTI battery analyser. The cell was charged at 4 $mA \cdot cm^{-2}$ for 20 minutes to an End of Charge Voltage (EoCV) of 2.6 V, allowed a two minutes open circuit period between charging and discharging, discharged at 4 $mA \cdot cm^{-2}$ to End of Discharge Voltage (EoDV) of 0.5 V for another 20 minutes, and allowed another open circuit two minutes. The EoCV was based on the SLFB cell voltage [4], while also allowing for over-potential. The EoDV was set low to ensure as complete a discharge cycle as possible. Each cell was cycled until the charge efficiency fell below 60%, at which point the cell was deemed to have failed.

The concentration of electrolyte was varied to investigate the effect of having different Pb^{2+} and acid concentrations. The RGE with the same MSA and Pb^{2+} ion concentration as the recovered electrolyte was cycled in the same cell. The results are reported in section 3.

2.4.3. Charge, Voltage and Energy Efficiency in Flow Cells

The performance of the electrolytes was further compared in a redox flow cell. The flow cell had an active electrode area of 10 cm^2, a VPX-20 anion membrane separator and an inter-cell gap of 2 cm either side of the membrane. The cell was connected to the MTI multi-channel battery analyser. 200 mL of the recovered electrolyte was placed in a tank (Erlenmeyer flask) and a Watson Marlow 505S peristaltic pump was used to circulate the electrolyte between the tank and the cell at 4.58 cm^3/s (2.29 cm/s). The setup is shown in Figure 3.

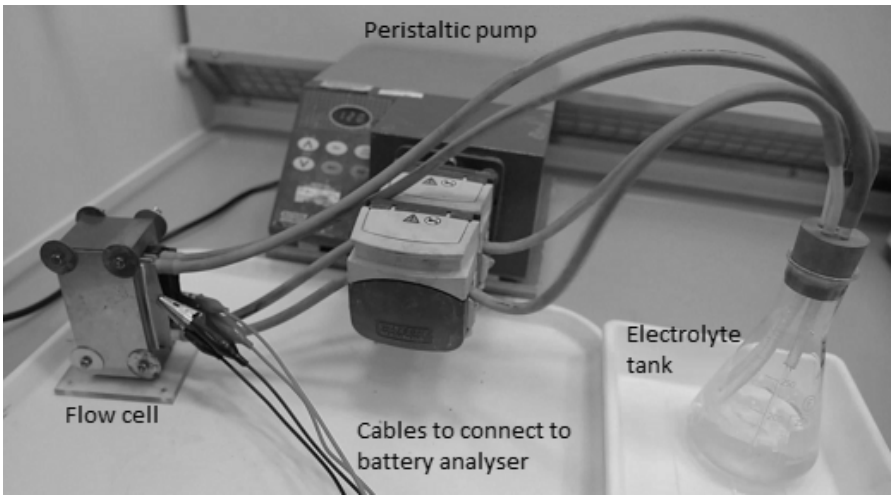

Figure 3: Setup of the redox flow cell, showing the redox flow cell in a vertical orientation, the Erlenmeyer flask as the electrolyte tank and peristaltic pumps. The cables connect the current collectors to the battery analyser.

The cell was charged at 10 $mA \cdot cm^{-2}$ to an EoCV of 2.6 V for one hour, allowed a two minutes open circuit period between charging and discharging, discharged at the same current

density to EoDV of 0.5 V for an hour, allowed another two minutes of open circuit, and the cycles were repeated until the cell charge efficiency fell below 60%, which was used to describe cell failure. The concentration of acid and Pb^{2+} ions was varied to compare, as was the current density. Reagent grade electrolyte with the same MSA and Pb^{2+} ion concentrations as the recovered electrolyte was cycled in the same fashion. The results are outlined in Table 3.

3. Results

3.1. Trace elements found in electrolyte

Trace elements found in recovered electrolyte using ICP – Mass Spectroscopy were silver, arsenic, bismuth, cadmium, copper, nickel, tin, antimony, beryllium, chromium, cobalt, magnesium, manganese, molybdenum, selenium, strontium, and tellurium. The first eight elements listed, along with zinc, are common elements found in refined lead ingots that conform to BS EN 12659:1999.

Figure 4 gives average quantities of three iterations of each sample for each element.

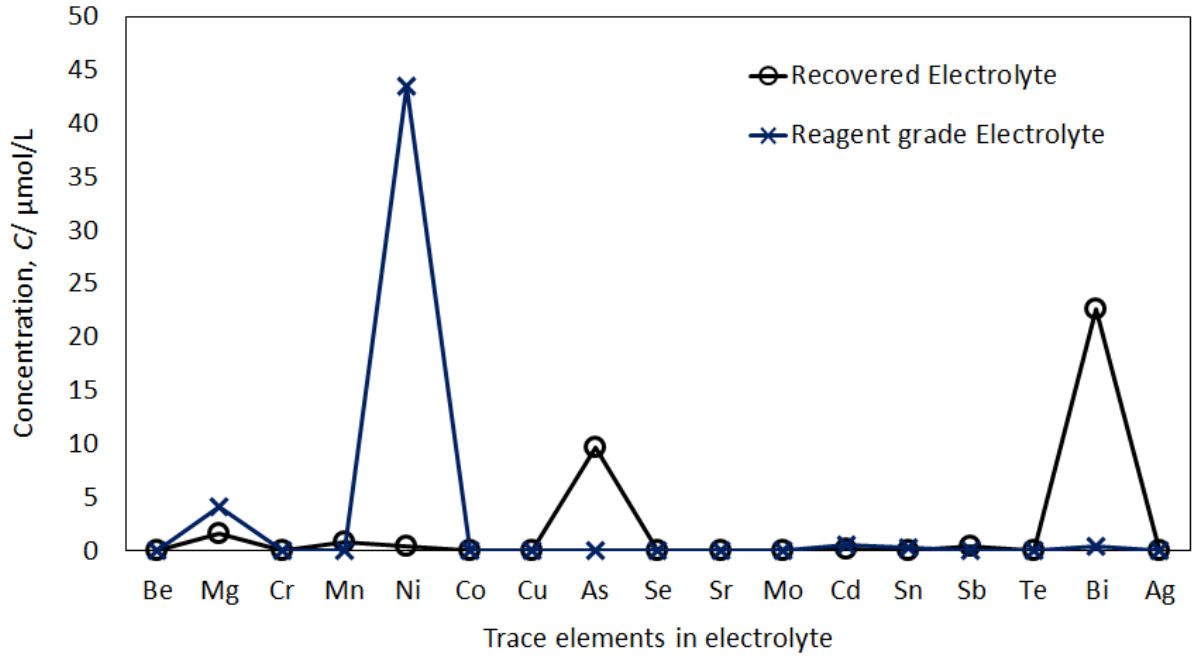

Figure 4: Trace elements found in samples of electrolyte made from lead acid battery electrodes. Samples were diluted and ionised using Argon plasma flame.

Figure 4 also shows that the highest concentrated impurity, nickel (43.5 µmol·dm^{-3}), is found in reagent grade electrolyte, and is 48% higher in concentration than the highest concentrated impurity, bismuth (22.7 µmol· dm^{-3}), found in recovered electrolyte. There are slightly elevated quantities of arsenic (12.0 µmol· dm^{-3}) and magnesium (1.6 µmol· dm^{-3}), for recovered electrolyte. The reagent grade electrolyte also has the highest concentration of magnesium, at 4.2 µmol·dm^{-3}.

3.2. Static Cells

Recovered electrolyte was cycled in the static cell shown in Figure 1. The cell was charged and discharged at 4 mA·cm^{-2} with a two minutes open circuit period between charging and discharging. The end of charge voltage was 2.6 V, while the end of discharge voltage was limited to 0.5 V. The reagent grade electrolyte was cycled in the static cell using the same cycling regime.

Figure 5 shows a comparison of the first two cycles of static cells running with recovered (RE) and reagent grade (RGE) electrolytes. It illustrates the difference in over-potential and in length of discharge period for the two cells. On charge, the voltage of the cell with RE is 0.25 V lower than that with RGE, while at the same time the RE discharge cycle is 6 minutes shorter than for the RGE cell. In cycle 2, the two cells run for the same length of time while the difference in voltage is maintained. Also clear is the two-stage charge profile on the second cycle, especially for the RGE cells, discussed later in the text.

In the first cycle the charge efficiency for the RGE cell was 78%, 13% higher than that for the RE, indicated by the 2 minute longer discharge period (Figure 5). In the second cycle both had risen to 90%. But the next twelve cycles, the charge efficiency for the RE stayed consistently above 90%, while that for the RGE cells dropped to 78% and continued on a steady decline until it fell below 60% after seven cycles. The voltage efficiency for the RGE cells averages 85% before cell failure. The average voltage efficiency of the RE cells was comparable at 86%.

Figure 6 shows subsequent cycles for the two cell types. From the fourth cycle, the RE cells have consistently longer discharge cycles, by at least six minutes longer than those of the reagent grade electrolyte cells, visible in cycles 5 and 6. This allowed for more capacity recovery during discharge and resulted in better charge efficiency, an average 90% compared to 78%. The RGE cells had energy efficiency from 77% at its highest to 51% at its lowest.

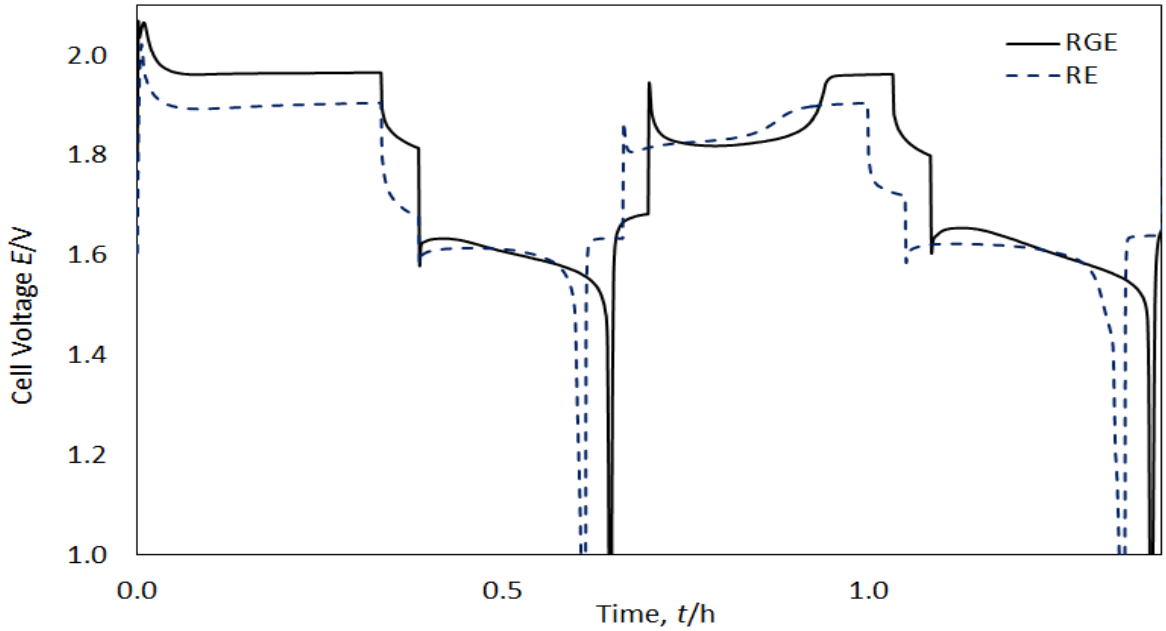

Figure 5: First 2 cycles of both recovered electrolyte (RE) and reagent grade electrolyte (RGE), ([Pb^{2+}]=0.9 mol·dm^{-3}) in static cell charged at 4 mA·cm^{-2} for 20 minutes to 2.6 V, left on open circuit voltage for 2 minutes, discharged at 4 mA·cm^{-2} for 20 minutes to 0.5 V, another 2 minutes on OCV and cycled until charge efficiency fell below 60% (failure).

Both Figure 5 and Figure 6 show that the charge/discharge curves start with over-potentials of 0.12 V for the RE cells and 0.14 V for the RGE cells. Both curves then adopt a flat charge profile in the first cycle, at 1.9 V and 1.96 V for the RE cells and RGE cells, respectively. These voltages, though slightly different are normal for converting Pb^{2+} is to solid PbO_2. Subsequent cycles show two voltage levels, 1.8 V and 1.9 V for RE cells and 1.85 V and 1.96 V for RGE cells. This phenomenon has been observed and studied by others [4, 5, 7, 18, 19] and it has been demonstrated that the shape of the curve is affected by activity at the positive electrode. The two-tiered charge voltages occur when an insoluble PbO_x (1>x>2) species is preferentially converted to PbO_2 at 1.8 V, before the conductive solid is depleted and Pb^{2+} is converted to solid PbO_2 at a voltage closer to 2.0 V [7]. Pletcher and Wills [6] concluded that the insoluble PbO_x species forms during discharge, when the boundary layer between the electrode and the electrolyte becomes saturated with Pb^{2+} ions beyond the solubility limit and the acid concentration at the electrode falls below the limit required to

convert PbO_2 to Pb^{2+}. Therefore, PbO_2 is converted to PbO_x instead [7]. Overtime, with more cycling, the undissolved lead dioxide becomes visible in the electrolyte, with both types of electrolytes, and on inspection after cycling, both types contain lead deposit on the negative electrode and lead dioxide on the positive electrode. The review by Krishna *et al.* [20] confirms this as the most prominent method of failure for the soluble lead battery. In undivided static cells, the growth of solids on both electrodes result in shorting of the circuit and failure of the cells much sooner than in divided cells.

In Figure 6, voltage instability due to the development of dendrites on the negative electrode is observed on cells with RGE first.

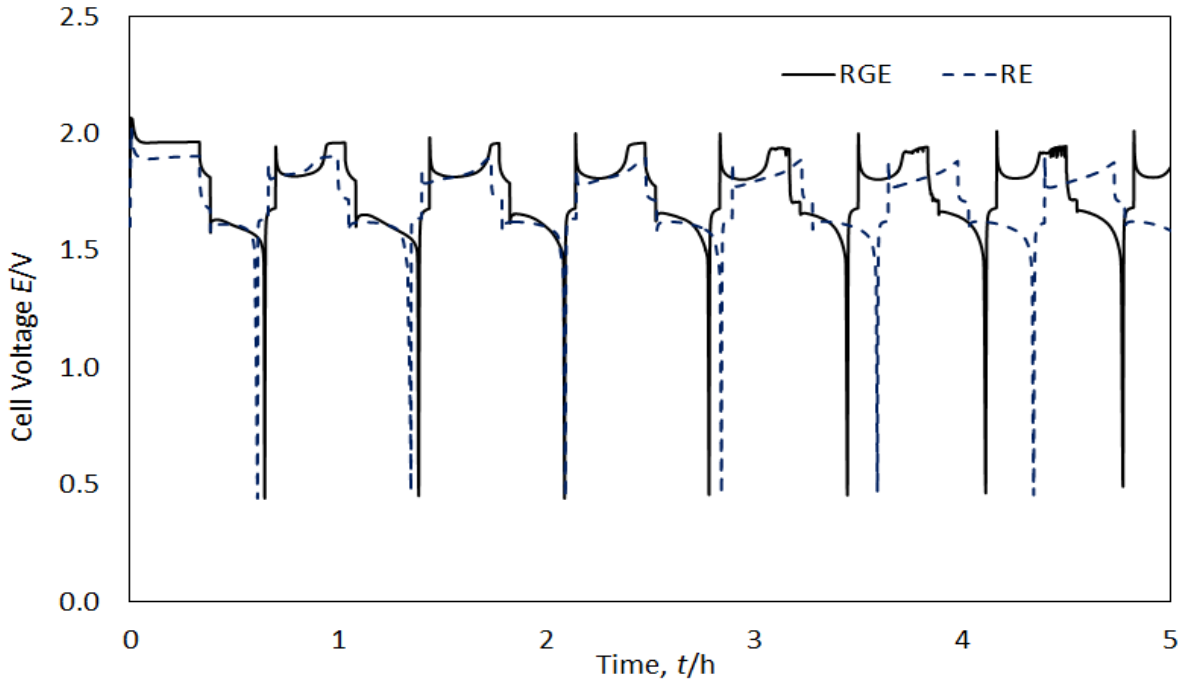

Figure 6: First 7 cycles of recovered electrolyte (RE) and reagent grade electrolyte (RGE) $[Pb^{2+}]$=0.9 mol·dm^{-3} in static cell charged at 4 mA·cm^{-2} for 20 minutes to 2.6 V, 2 minutes on open circuit voltage (OCV), discharged at 4 mA·cm^{-2} for 20 minutes to 0.5 V, another 2 minutes on OCV. Cycled until charge efficiency fell below 60% (failure).

Table 2 presents a comparison of cells operating on the two electrolytes at similar Pb^{2+} concentrations. In all cases the cells with recovered electrolyte cycled more times before the charge efficiency fell below 60%. The charge and energy efficiencies for the cells with recovered electrolyte were also consistently higher than that using reagent grade electrolyte. The charge efficiency of the cells with recovered electrolyte was consistently higher than 80%, while that of the lab reagent electrolyte cells peaked at 74%. Table 2 indicates that in the static cell, the recovered electrolyte overall produced an improved cell performance and cycle life than the cells using the reagent grade electrolyte.

Table 2: Average performance of static cells using recovered (RE) and reagent grade (RGE) electrolytes. The static cell had an active electrode area of 25 cm^2 and was cycled at 4 $A \cdot cm^{-2}$ for 20 minutes to EoCV of 2.6 V, allowed to rest and discharged at 4 $A \cdot cm^{-2}$ for 20 minutes to EoDV of 0.5V.

Electrolyte	$[Pb^{2+}]$ / $mol \cdot dm^{-3}$	Charge Efficiency /%	Energy Efficiency /%	Voltage Efficiency /%	Cycles to Failure*
1 RE	1.0	89	86	96	23
2 RGE	1.0	63	49	78	7
3 RE	0.9	89	77	87	17
4 RGE	0.9	74	63	85	8

* Failure is defined when the charge efficiency fell below 60%.

3.3. Redox Flow Cells

The redox flow cell shown in Figure 2 was charged at 20 $mA \cdot cm^{-2}$ for one hour to an EoCV of 2.6 V, allowed a two minutes open circuit period between charging and discharging,

discharged at 20 mA·cm^{-2} to an EoDV of 0.5 V, allowed another 2 minutes. Cycles were repeated until charge efficiency fell below 60%, at which time they were deemed to have failed. The electrolyte flow was 4.58 cm^{3}·s^{-1} (2.29 cm·s^{-1}). The cell had 10 cm^{2} carbon polymer negative and positive electrodes, an anion permeable membrane VPX-20, a 2 cm gap between the membrane and either electrode and 0.5 mm thick nickel foil current collectors. Performance of the recovered electrolyte is compared to that of reagent grade electrolyte cycled in the same cell, and the results are shown in Table 3.

Table 3: Average performance of recovered (RE) and reagent (RGE) grade electrolyte in a soluble lead redox flow cell charged at 10 mA·cm^{-2} for an hour to EoCV of 2.6V, 2 minutes OC and discharged at 10 mA·cm^{-2} to EoDV 0.5 V. Cell failure defined when charge efficiency fell below 60%.

Electrolyte	[Pb^{2+}] /mol·dm^{-3}	Current density /mA·cm^{-2}	Charge Efficiency /%	Energy Efficiency /%	Voltage Efficiency /%	Cycles before Failure
1 RE	0.9	10	88	68	77	47
2 RGE	0.9	10	88	65	74	56
3 RE	0.9	20	80	55	69	98
4 RGE	0.9	20	87	63	72	102
5 RE	0.7	10	84	66	79	187
6 RGE	0.7	10	78	63	81	101

The charge efficiency displayed by the cell using recovered electrolyte is similar to that of the cell using electrolyte made from laboratory reagents. The similarity can be seen in both the static cell, (Table 2) and the flow cell (Table 3). It is also evident at different current densities. The voltage efficiency of cells with either electrolyte is also comparable. The

number of cycles supported by the recovered electrolyte in a redox flow cell is significantly higher (86 cycles more) at a Pb^{2+} ion of 0.7 mol· dm^{-3} and 1.0 mol· dm^{-3} MSA, which was recommended for optimum electrochemical performance of a soluble lead cell [14].

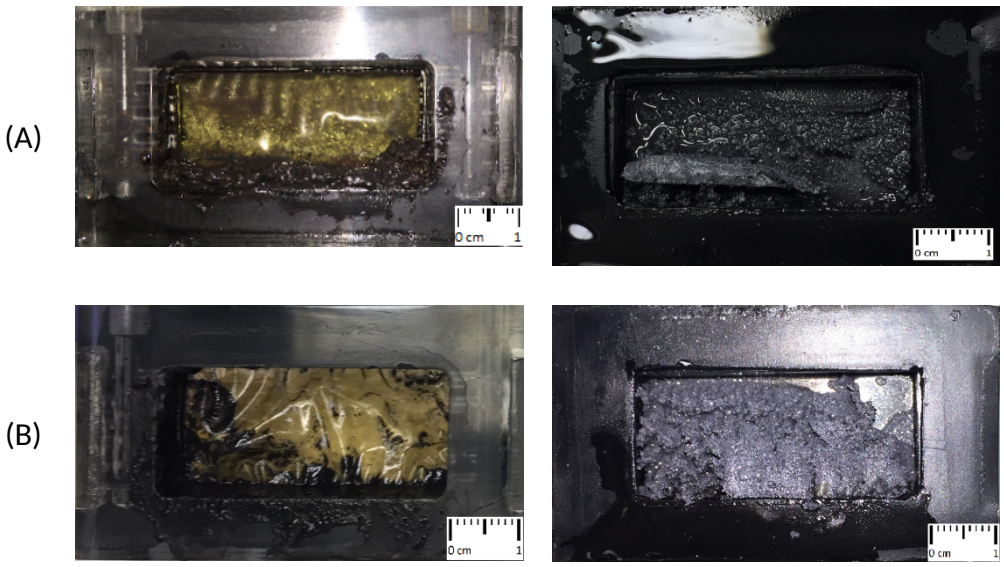

Figure 7: Solid build-up in positive (left) and negative (right) half cells of a soluble lead redox flow cell after 7 days of cycling at 10 mA·cm^{-2} on 1 hour charge and discharge cycles with 2 minutes of open circuit pauses between cycles. (A) depicts deposit for a flow cell with reagent grade electrolyte recovered electrolyte and (B) shows deposit build-up for a cell using.

When left to continue to cycle, formation of solid deposit occurred in cells with either electrolyte, as shown in Figure 7. A shiny spongy lead was deposited on the negative electrode while a sludgy and grainy deposit was formed in the positive half-cell. After seven days, not only has the deposit grown to fill the cell chamber, the surface of the deposit is no longer smooth. Inefficient reduction of lead dioxide, which starts with deposition of the PbO_x during discharge, results on the accumulation of lead dioxide on the positive electrode. In turn lead starts to accumulate on the negative electrode. In a divided cell, as long as there is no contact between the growing solids, the cell continues to operate at charge efficiencies above 80%, even as the black lead dioxide can be seen in the electrolyte tank. Similar results

were observed by Li *et al*. [13]. However with increased cycling the deposits grow until the negative side of the cell fills with soft spongy lead (Figure 7) while the lead dioxide continues to travel with electrolyte to the tank. Eventually the Pb^{2+} concentration in the electrolyte falls too low as more lead is deposited and not stripped back into the electrolyte.

The charge discharge cycles at 18 $mA \cdot cm^{-2}$ for both electrolytes are shown in Figure 8. Over-potential starts high for both flow cells, indicating initially high losses. The difference between the charge and discharge voltages gradually lessens, improving voltage efficiency and the charge efficiency, which tends towards 90% for both electrolytes. Another noticeable feature of the curve in Figure 8 is that the over-potential for the recovered electrolyte is less than that of the reagent grade electrolyte, even as they both decrease with cycling. This means less energy is required to charge the cell with recovered electrolyte than is required for that with reagent grade electrolyte.

Figure 8 also indicates that the first cycle of the RE cell immediately displays almost equal charge and discharge times, while also being fairly flat, compared to the RGE flow cell. This signals the high charge efficiency at the onset of cycling, which was recorded as 90% in the first cycle, while the RGE cell charge efficiencies start at 70% and gradually increase. At failure, defined when charge efficiency fell below 60%, both cells had an average charge efficiency of 84%.

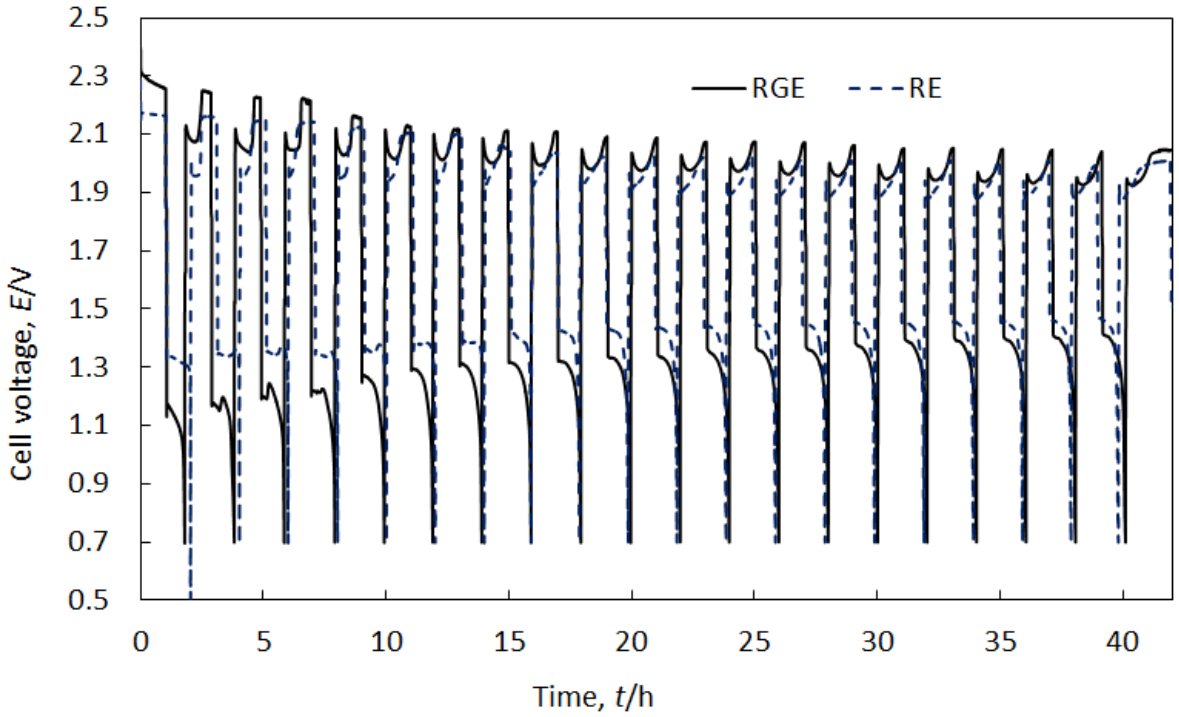

Figure 8: Comparison of recovered (RE) and reagent grade electrolytes (RGE) cycled in a RFC at 18 mA·cm^{-2}. The cell was charged for an hour, left on open circuit for 2 minutes, discharged for an hour, and allowed another 2 minutes. EoCV: 2.6 V & EoDV: 0.5 V. The curves show a gradual decrease in over-potentials, which occurs earlier for the recovered electrolyte.

As with static cell cycles, the graph indicates that subsequent charge occurs at two different voltages. In the second cycle, charge is initially at 2.1 V then at 2.3 V, similar to the static cell performance in section 33.2.

4. Discussion

Section 3.2 indicates that, in the static cell with 1.0 mol·dm^{-3} Pb^{2+}, the recovered electrolyte had 89% charge, 86% energy and 96% voltage efficiency compared to 63%, 49% and 78% charge, energy and voltage efficiencies, respectively, for the reagent grade electrolyte. In commercial lead acid batteries, the presence of tin on the positive electrode has been credited with preventing electrode passivation due to the formation of resistive PbO on the electrode surface [21, 22]. Tin corrosion layers have also been credited with a higher

conductivity than the pure lead deposit that would normally be made [17]. Compared to 0.5 mol·dm^{-3} (<2% w/w) used in the conventional lead acid battery, the 8.6 μmol·dm^{-3} tin content in the recovered electrolyte was low, and therefore its effect expected to be low, especially since the anti-passivation effects on lead acid batteries improve with higher amounts of the tin additive [21, 22]. However, it is possible that before the Sn^{2+} ions are depleted, they enhance the adhesion of deposit on the positive electrode, ensuring that the cell using recovered electrolyte performs better in the first cycle.

Wallis and Wills [23] used a bismuth additive on a divided static cell, and found a 20 fold improvement in cell cycle life. They added 10 mmol·dm^{-3} Bi^{3+} to electrolyte at the positive electrode and observed an improvement on the stripping peak of lead dioxide, which tended to flatten and broaden with cycling beforehand. They also observed a shift in the equilibrium potential for the PbO_2/Pb^{2+} couple from 1.440 V vs SCE at 0% content to 1.651 V vs SCE at 20 mmol·dm^{-3} Bi^{3+} [23]. Since the stripping peak of PbO_2 tends towards more negative values with cycling, adding Bi^{3+} improved the coulombic efficiency of the couple. Bismuth is also credited with improving contact and therefore conductivity between PbO_2 particles in a lead acid battery. For the RE under consideration, the amount of bismuth averaged 22.7 μmol·dm^{-3}, which is considerably lower than the quantities used by Wallis and Wills. Nonetheless the benefits of its presence cannot be discounted, especially if there are tandem benefits to having other impurities in the electrolyte.

The effects of nickel additive on an undivided soluble lead cell were highlighted by Hazza *et al.* [8] where they showed that nickel had a detrimental effect on charge efficiency. They found that even at 0.1 g·dm^{-3}, nickel lowered the cell charge efficiency by 12%, and

increasing nickel content led to worse results. The reagent grade electrolyte had the highest nickel content of 43.5 μmol·dm^{-3} and this could account for the lower charge efficiencies observed for cells using reagent grade electrolyte, especially in the static undivided cells. Performance of the recovered electrolyte is comparable to that of the reagent grade electrolyte in the flow cell. Cells with either electrolyte have columbic efficiencies close to or above 80%. For the recovered electrolyte flow cell, high coulombic efficiencies above 90% are reached at the first cycle. At larger scale, this could provide instantaneous large energy discharge for MW applications.

The tendency towards two-stage charge voltage after the first cycle was observed for both electrolytes in both the static and the flow cells. This behaviour is due to formation of solid PbO or PbO_x at the positive electrodes during charge [4, 5, 7, 18, 24]. During discharge, solid PbO/PbO_x is converted to Pb^{2+} ions at 1.8 V first, before PbO_2 is at 2.0 V. This creates the two discharge voltage levels. This phenomenon contributes to the eventual build-up of solids on both electrodes and affects cells with both electrolytes. It evidences the similarity of the two electrolytes and confirms that the two can be used interchangeably.

5. Conclusions and Further Work

The performance of recovered electrolyte was demonstrated in an undivided static soluble lead cell with 25 cm² carbon polymer electrodes, where the charge efficiency of the cell was consistently above 80% (Table 2), achieving better performance than that of an equivalent cell using electrolyte prepared from reagent grade chemicals. Performance in a flow system was also confirmed in a semi-divided (one tank) soluble lead redox flow cell with 10 cm² carbon polymer electrodes and an anion exchange membrane. Charge efficiency in this cell

also stayed consistently above 80%, reaching an average of 90% in some instances. The number of cycles before charge efficiency fell below 60% was lower for reagent grade electrolyte static cells, and comparable for flow cells, except at 0.7 mol·dm^{-3} Pb^{2+} where the cell with recovered electrolyte cycled for 187 cycles compared to the reagent grade electrolyte cells' 102 cycles. Based on the performance displayed in both types of cells, the recovered electrolyte appears to be a viable option to the reagent grade electrolyte, which provides a financially attractive option to sourcing materials for the soluble lead redox flow battery.

Even though the recovered electrolyte is made from end-of-life lead acid battery electrodes, ICP-Mass Spectroscopy has revealed that the impurities found in the electrolyte are minute, and in some cases lower in concentration than those found in reagent grade electrolyte. Nickel is a case in point, found at 43.5 µmol·dm^{-3} in RGE and at almost zero percent in RE. However the performance of the recovered electrolyte is undeniably attractive and it is possible that the trace elements found in the electrolyte work in tandem to benefit cells containing this electrolyte. Future work will investigate the effects of these impurities individually and together. Future work will also include investigation of all the other impurities found in the recovered electrolyte, as well as identification and investigation of effects of organic impurities in the recovered electrolyte.

Insoluble solid sludge accumulation in the positive side of the cells, which was then carried along with the electrolyte to the tank was observed for both electrolytes, while in the negative side, a spongy mass of lead accumulated on the negative electrode, shown in Figure 7. Therefore for both electrolytes, the biggest challenge to the soluble lead battery is inefficient reduction of lead dioxide, which ultimately starts the accumulation of solids

inside the cell and leads to failure. More work needs to go into improving the kinetics of the PbO_2/Pb^{2+}couple and improving the stripping efficiency of PbO_2. Future work also includes further investigation of deposit morphology to determine its effect on growth and accumulation of solids inside the cell.

Acknowledgements

The research leading to this paper was financially supported by the Government of Botswana and the Botswana International University of Science and Technology (BIUST).

References

1. Teller, O., et al., *Joint EASE/EERA recommendations for a European energy storage technology development roadmap towards 2030*, Martens, D., Editor. 2013, European Association for Storage of Energy (EASE) and European Energy Research Alliance (EERA): Brussels, Belgium. p. 1-226.[Acessed on: 25/09/2014].
2. Ponce de León, C., et al., *Redox flow cells for energy conversion.* Journal of Power Sources, 2006. **160**(1): p. 716-32.DOI: http://dx.doi.org/10.1016/j.jpowsour.2006.02.095.
3. Vanýsek, P. and Novák, V., *Redox flow batteries as the means for energy storage.* Journal of Energy Storage, 2017. **13**: p. 435-41.DOI: https://doi.org/10.1016/j.est.2017.07.028.
4. Hazza, A., Pletcher, D., and Wills, R., *A novel flow battery: A lead acid battery based on an electrolyte with soluble lead(ii) Part I. Preliminary studies.* Physical Chemistry Chemical Physics, 2004. **6**(8): p. 1773-8.DOI: 10.1039/B401115E.
5. Pletcher, D. and Wills, R., *A novel flow battery: A lead acid battery based on an electrolyte with soluble lead(ii) Part II. Flow cell studies.* Physical Chemistry Chemical Physics, 2004. **6**(8): p. 1779-85.DOI: 10.1039/B401116C.
6. Pletcher, D., Hazza, A., and Wills, R., *A novel flow battery-A lead acid battery based on an electrolyte with soluble lead(II).* Journal of Power Sources, 2005. **149**: p. 103-11.DOI: 10.1016/j.jpowsour.2005.01.049.
7. Pletcher, D. and Wills, R., *A novel flow battery - A lead acid battery based on an electrolyte with soluble lead(II) - III. The influence of conditions on battery performance.* Journal of Power Sources, 2005. **149**: p. 96-102.DOI: 10.1016/j.jpowsour.2005.01.048.
8. Hazza, A., Pletcher, D., and Wills, R., *A novel flow battery - A lead acid battery based on an electrolyte with soluble lead(II) - IV. The influence of additives.* Journal of Power Sources, 2005. **149**: p. 103-11.DOI: 10.1016/j.jpowsour.2005.01.049.
9. Pletcher, D., et al., *A novel flow battery - A lead-acid battery based on an electrolyte with soluble lead(II) V. Studies of the lead negative electrode.* Journal of Power Sources, 2008. **180**(1): p. 621-9.DOI: 10.1016/j.jpowsour.2008.02.024.
10. Pletcher, D., et al., *A novel flow battery - A lead-acid battery based on an electrolyte with soluble lead(II) Part VI. Studies of the lead dioxide positive electrode.* Journal of Power Sources, 2008. **180**(1): p. 630-4.DOI: 10.1016/j.jpowsour.2008.02.025.
11. Wills, R. *A lead acid flow battery for utitlity scale energy storage and load levelling*. 2004. PhD, University of Southampton.
12. Gernon, M., et al., *Environmental benefits of methanesulfonic acid . Comparative properties and advantages.* Green Chemistry, 1999. **1**(3): p. 127-40.DOI: 10.1039/A900157C.
13. Li, X., Pletcher, D., and Walsh, F.C., *A novel flow battery: A lead acid battery based on an electrolyte with soluble lead(II) Part VII. Further studies of the lead dioxide positive electrode.* Electrochimica Acta, 2009. **54**(20): p. 4688-95.DOI: 10.1016/j.electacta.2009.03.075.
14. Krishna, M., et al., *Measurement of key electrolyte properties for improved performance of the soluble lead flow battery*. International Journal of Hydrogen Energy, 2017.DOI: https://doi.org/10.1016/j.ijhydene.2017.05.004.
15. Pavlov, D., *Chapter 14 - Methods to Restore the Water Decomposed During Charge and Overcharge of Lead–Acid Batteries. VRLA Batteries*, in *Lead-Acid Batteries: Science and Technology*. 2011, Elsevier: Amsterdam. p. 567-603.ISBN: 978-0-444-52882-7.
16. Orapeleng, K., Wills, R., and Cruden, A., *Developing Electrolyte for a Soluble Lead Redox Flow Battery by Reprocessing Spent Lead Acid Battery Electrodes.* Batteries, 2017. **3**(2): p. 15.DOI: 10.3390/batteries3020015.
17. Prengaman, R.D., *Chapter 2 - Lead Alloys for Valve-regulated Lead-Acid Batteries*, in *Valve-Regulated Lead-Acid Batteries*, Rand, D.A.J., et al., Editors. 2004, Elsevier: Amsterdam. p. 15-35.ISBN: 978-0-444-50746-4.

18. Collins, J., et al., *A novel flow battery: A lead acid battery based on an electrolyte with soluble lead(II) Part VIII. The cycling of a 10 cm x 10 cm flow cell.* Journal of Power Sources, 2010. **195**(6): p. 1731-8.DOI: 10.1016/j.jpowsour.2009.09.044.
19. Oury, A., Kirchev, A., and Bultel, Y., *Oxygen evolution on alpha-lead dioxide electrodes in methanesulfonic acid.* Electrochimica Acta, 2012. **63**(0): p. 28-36.DOI: http://dx.doi.org/10.1016/j.electacta.2011.12.028.
20. Krishna, M., et al., *Developments in soluble lead flow batteries and remaining challenges: An illustrated review.* Journal of Energy Storage, 2018. **15**: p. 69-90.DOI: https://doi.org/10.1016/j.est.2017.10.020.
21. Li, D., et al., *Effect of Sn content on the properties of passive film on PbSn alloy in sulfuric acid solution.* Science in China Series B: Chemistry, 2007. **50**(4): p. 501-4.DOI: 10.1007/s11426-007-0091-z.
22. Matteson, S. and Williams, E., *Residual learning rates in lead-acid batteries: Effects on emerging technologies.* Energy Policy, 2015. **85**: p. 71-9.DOI: http://dx.doi.org/10.1016/j.enpol.2015.05.014.
23. Wallis, L.P.J. and Wills, R.G.A., *Membrane divided soluble lead battery utilising a bismuth electrolyte additive.* Journal of Power Sources, 2014. **247**: p. 799-806.DOI: http://dx.doi.org/10.1016/j.jpowsour.2013.09.026.
24. Oury, A., et al., *PbO2/Pb2+ cycling in methanesulfonic acid and mechanisms associated for soluble lead-acid flow battery applications.* Electrochimica Acta, 2012. **71**(0): p. 140-9.DOI: http://dx.doi.org/10.1016/j.electacta.2012.03.116.